

Journal of Materials Chemistry A

Accepted Manuscript



This is an *Accepted Manuscript*, which has been through the Royal Society of Chemistry peer review process and has been accepted for publication.

Accepted Manuscripts are published online shortly after acceptance, before technical editing, formatting and proof reading. Using this free service, authors can make their results available to the community, in citable form, before we publish the edited article. We will replace this *Accepted Manuscript* with the edited and formatted *Advance Article* as soon as it is available.

You can find more information about *Accepted Manuscripts* in the [Information for Authors](#).

Please note that technical editing may introduce minor changes to the text and/or graphics, which may alter content. The journal's standard [Terms & Conditions](#) and the [Ethical guidelines](#) still apply. In no event shall the Royal Society of Chemistry be held responsible for any errors or omissions in this *Accepted Manuscript* or any consequences arising from the use of any information it contains.

Dealloyed PtCo Hollow Nanowires with Ultrathin Wall Thicknesses and Their Catalytic Durability for the Oxygen Reduction Reaction

Cite this: DOI: 10.1039/x0xx00000x

Received 00th January 2012,
Accepted 00th January 2012

DOI: 10.1039/x0xx00000x

www.rsc.org/

Yan Huang,^{*a} Miguel Garcia,^a Syed Habib,^a Jianglan Shui,^a Frederick T. Wagner,^b Junliang Zhang,^{b,†} Jacob Jorné,^a and James C.M. Li^a

The poor durability and high cost of Pt nanoparticles has always been a challenge to the commercialization of proton exchange membrane fuel cell (PEMFC)-powered vehicles. Pt-based nanowires have better durability and catalytic activity. Hollow nanowires reduce Pt consumption and thus save cost. In this paper, PtCo hollow nanowires with well-controlled ultrathin wall thicknesses of 2–4 nm have been synthesized by electrospinning, annealing and dealloying. To our best knowledge, these are the thinnest wall yet achieved by use of electrospinning. The mechanism of hollow nanowire evolution is studied. It is found that the temperature of reduction is crucial for the retention of the hollow structure. In contrast to conventional Pt/C nanoparticles which lose 38% of their initial activity, these ultrathin hollow nanowires exhibit well-preserved activities after 10000 cycles. Our studies raise promising possibilities for synthesizing highly durable Pt-based catalysts.

Introduction

Industrial applications of polymer electrolyte membrane fuel cells (PEMFCs)^[1–3] are limited by the slow kinetics of oxygen reduction reaction (ORR).^[4–9] Pt nanoparticles are the major active materials for ORR electrocatalysis.^[10–13] In attempts to increase ORR activities, a number of novel structures have been prepared and tested, including Pt-based nanoparticles supported on mesoporous carbons with various compositions,^[5,14,15] shape-controlled particles,^[14,16] and core-shell structures.^[17–21] However, poor durability and high cost remain major problems.^[22,23] Due to the high surface energy of nanoparticles, they tend to grow and aggregate resulting in the loss of surface area.^[24–27] Pt-based nanowires and nanorods have better durability and enhanced activities compared to carbon-supported Pt nanoparticles.^[28–45]

There are a number of ways reported to make one-dimensional nanowire structures, such as copper underpotential deposition,^[37] chemical reduction,^[46,47] chemical vapor deposition,^[48] template method,^[38,49] electrospinning,^[32,50,51] etc. Among these methods, electrospinning is a facile way to make an interweaving network of long wires (millimeters in length)^[32,50–56] while avoiding particle agglomeration.^[32,50,51] In

addition, hollow nanowires have been obtained by heating solid precursor nanowires from electrospinning.^[57] The hollow structure can provide lower Pt consumption and thus save cost, and may even improve catalytic performance.^[58,59] However, the wall is too thick (15–20 nm)^[57] to effectively utilize materials.

In this paper, we report dealloyed PtCo hollow nanowires with ultrathin wall thickness (2–4 nm) formed by a single electrospinning step followed by annealing and dealloying. This is the thinnest size of wall reported to our best knowledge by using the same or a similar method. The temperature of reduction is found to be crucial for the maintenance of the hollow structure. These long, ultrathin hollow nanowires exhibit far better durability and higher ORR activities than conventional Pt/C nanoparticles.

Results and discussion

PtCo₂ hollow nanowires of 40–50 nm diameter formed a network after annealing in air. These wires were too long to be measured (Figure 1a, b). After 5 h reduction in H₂ at 250 °C, the wire diameter decreased to 30–40 nm while the hollow structure was maintained (Figure 1c, d). It can be clearly seen

that the wall is uniform and the thickness is around 5 nm (Figure 1e). HAADF (Figure 1f) and elemental linear scans along a cross section by energy-dispersive spectroscopy (EDX) (inset in Figure 1f) confirmed the hollow structure. Both Pt and Co have highest peaks on the edges, and also lowest ones along the center of the wire. Their spectra overlay, indicating a homogeneous distribution of Pt and Co atoms, *i.e.*, PtCo alloys.

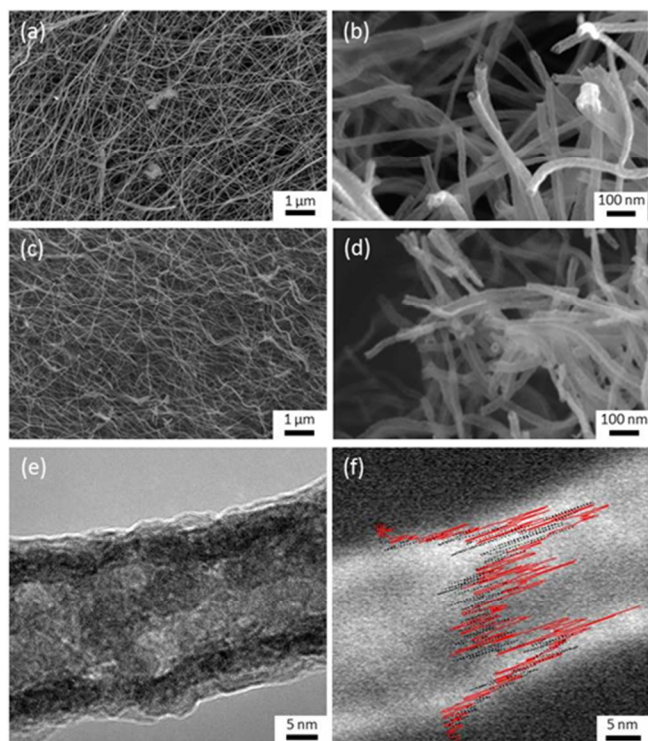


Figure 1. (a,b) SEM images of PtCo₂ hollow nanowires after annealing in air up to 500 °C, (c,d) SEM images, (e) TEM and (f) HAADF of PtCo₂ hollow nanowires after reduction at 250 °C for 5 h (inset is a cross-sectional compositional line profile: Pt (solid red) and Co (dashed black)).

X-ray diffraction patterns before and after reduction are shown in Figure 2, indicating that almost all of the Co were in the form of an oxide after annealing in air and the Pt was in a noncrystalline form. After reduction in H₂, the only observed phases were PtCo alloys and Pt. The transition from oxide to metal explains the size contraction upon reduction (Figure S1).

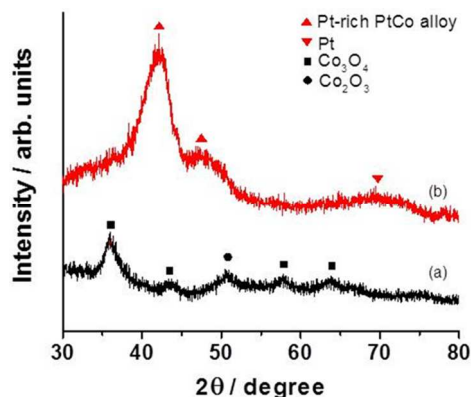
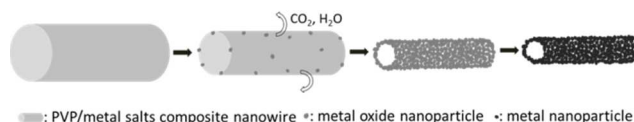


Figure 2. X-ray diffraction of PtCo₂ hollow nanowires after (a) annealing in air up to 500 °C, and (b) subsequent 5 h reduction in H₂ at 250 °C.

The electron microscopy and XRD results lead us to hypothesize that there are several stages in the hollow wire formation process: (a) Electrospinning generated a solid composite wire of polymer and metal salts (see the as-spun composite wires in Figure S2). (b) Heat treatment in air oxidized the polymer (to CO₂, water, N₂, et. al.) and the salts from the surface inwards, initially forming metal oxide nanoparticles dispersed within remaining unoxidized polymer. As oxidation of the polymer progressed further, the oxide particles gradually got connected and formed a rigid, porous wall which fixed the diameter of the oxidized wire. (c) Since the wall was porous, it allowed oxygen to diffuse in to oxidize the polymer and the metal salt inside. The vaporized water and CO₂ diffused out and metal oxide was deposited inside next to the wall or within the wall, forming a hollow wire. When the oxidation process finished, the wire was completely hollow with a wall thickness that is believed to depend on the initial polymer concentration and the oxidation temperature. (d) In the reduction stage, porosity allowed hydrogen to reduce the oxide to metal, leading to shrinkage of the wire diameter. This process is shown in Scheme 1.



Scheme 1. Formation of the hollow PtCo structure starting from as-spun composite nanowires.

Chen et al. studied the morphology evolution comprehensively until the step of oxidation.^[57] Morphologies under different reduction temperatures were studied here (Figure 3a,b). At 350 °C, hollow nanowires seemed to be melted a bit, leaving some pores on the surface. When the temperature increased to 450 °C, nanowires turned to be beads-connected without the hollow structure. These show that the reduction temperature needs to be well controlled in order to keep hollow nanowires. The microstructure of PtCo alloy might be also influenced by the annealing temperature, although the average composition of PtCo alloy (1:2) does not change.

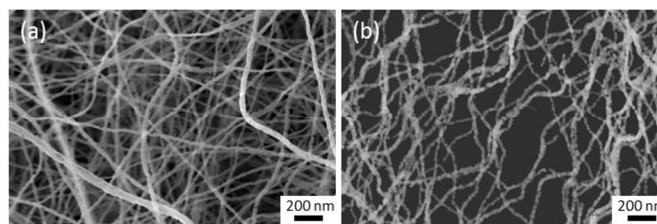


Figure 3. SEM images of PtCo₂ nanowires after 5 h reduction in H₂ at (a) 350 °C, and (b) 450 °C.

By use of similar techniques (electrospinning and heat treatment), Chen et al.^[57] obtained similar hollow nanowires of iron and cobalt oxide. Li et al.^[49] also prepared tubes of some cobalt oxides by annealing in air. However, the wall thickness

of our hollow nanowires was the thinnest achieved to our best knowledge by using the same or similar method.^[60-63]

After acid leaching in 1 M HNO₃ at 80 °C for 5 h, the nanowire size had further decreased to 20~30 nm meanwhile the network was well kept (Figure 4a). Atomic ratio of Pt:Co changed from 1:2 initially to 1.4:1 by SEM EDX measurement (Figure 4b). A clearer morphology with lattice fringes can be seen in the TEM image (Figure 4c). The wall thickness was only 2~4 nm. The surface is mainly composed of (111) atomic plane of pure metallic Pt, with only a few of alloyed PtCo. This indicates that most surface Co atoms have been removed by acid leaching. This desired core-shell structure (*i.e.*, Pt-rich surface and PtCo alloy underneath the surface) is to resemble the Pt-skin Pt_xM bimetallic alloy nanostructures reported^[64] to have enhanced activity and durability. We chose a 5 h acid leach because longer dealloying times caused the wires to curve, although their diameter didn't change much (Figure S3) and thus the composition and resulted activity are believed to be close under longer dealloying durations.

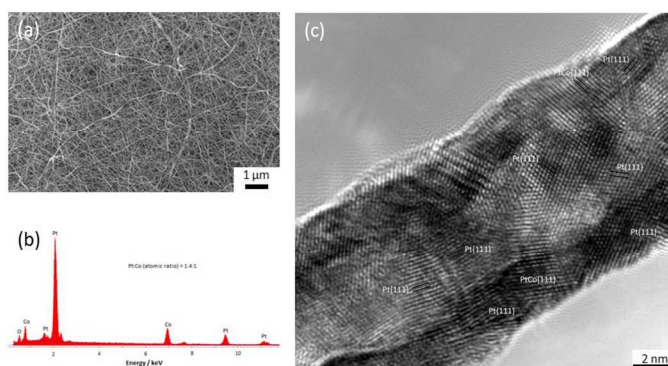


Figure 4. (a) SEM image, (b) EDX spectrum, and (c) TEM image of hollow PtCo ultrathin nanowires after acid leaching in 1 M HNO₃ at 80 °C for 5 h.

Durability test was conducted by cycling the RDEs in N₂-saturated dilute electrolyte (0.1 M HClO₄) 10000 times from 0.6 to 1.0 V vs. RHE at a sweep rate of 50 mV s⁻¹ at room temperature (Figure 5). It can be seen from Figure 5a that CVs before and after cycling overlay well. The electrochemical surface area is 26 m² g⁻¹_{Pt}, which is, as expected, about half of that seen for conventional nanoparticulate Pt/C (53.8 m² g⁻¹_{Pt}).^[65] Importantly, the ORR polarization curve is also well retained after 10000 cycles (Figure 5b). There is nearly no change either in the half wave potential or in the diffusion current of the polarization curve, suggesting that there is neither activity loss nor obvious composition change. This is superior to most cycling stabilities of Pt-based electrocatalysts reported. The morphology was well maintained and no obvious composition change was observed after the cycling test for many small Pt-based nanowires (maximum μm in length).^[40,42,66-74] Our PtCo hollow nanowires are ultralong (in the magnitude of mm) and the wire diameter is large (20-30 nm). More importantly, they form a self-interweaving network. Therefore, the excellent durability is believed to arise- from the stable long-interweaving nanowires, which do not undergo significant agglomeration or Ostwald ripening.^[32,37,75] By comparison, commercial Pt/C nanoparticles lose 38% of specific activity and 25% of mass activity after 10000 cycles (Figure 5c,d). The rapid decline of activities for Pt/C results from the agglomeration, Pt dissolution and ripening of nanoparticles.^[24-27,37,76] It should be noted that PtCo/C

nanoparticles have a close specific activity (~700 μA/cm²_{Pt}) and higher mass activity (0.34 A/mgPt) than PtCo hollow nanowires and Pt/C nanoparticles,^[65] but their cycling stability is similar to Pt/C nanoparticles due to the same reasons of nanoparticle agglomeration and ripening mentioned above.^[1,77-82] It is also noteworthy that the activities of PtCo hollow nanowires are higher than those of Pt/C and also other nanowires such as Pt nanotubes,^[83] star-like Pt nanowires,^[84] porous PtFe nanowires,^[32] etc. The activity enhancement could arise from several sources. The continuous nanowires are curved in only one direction, while nanoparticles are curved in all directions. Therefore the mean coordination number of the surface Pt atoms is expected to be higher for continuous nanowires vs. nanoparticles, decreasing the bonding strength of O-containing adsorbates and increasing ORR activity.^[1] The presence of the Co alloying element can also increase the activity. Figure 4c shows the presence of lattice fringes corresponding to (111) planes of PtCo and Pt. These catalysts partially benefit from the very high activity previously seen for (111) planes of large Pt-alloy crystals.^[5]

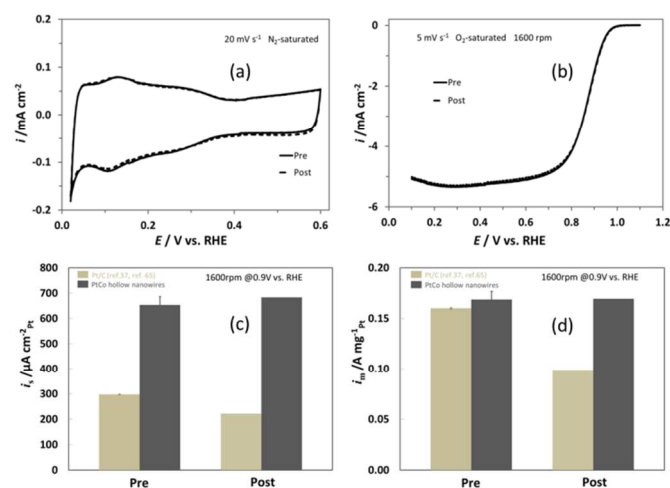


Figure 5. (a) CV curves of dealloyed hollow PtCo ultrathin nanowires recorded at 0 and 10000 cycles in N₂-saturated 0.1 M HClO₄ solution at a sweep rate of 20 mV s⁻¹, (b) ORR polarization curves of dealloyed hollow PtCo ultrathin nanowires recorded at 0 and 10000 cycles in O₂-saturated 0.1 M HClO₄ solution at a sweep rate of 5 mV s⁻¹, a rotation speed of 1600 rpm, (c) specific activities, and (d) mass activities of dealloyed hollow PtCo ultrathin nanowires at 0.9 V versus RHE, in comparison with those of Pt/C calculated from refs. 37 and 65.

Experimental

Synthetic procedures. A precursor solution was prepared using polyvinylpyrrolidone (50 mg ml⁻¹, PVP, 1.3×10⁶ MW, Aldrich), hexachloroplatinic acid (15 mM, H₂PtCl₆•6H₂O, Aldrich), cobalt nitrate (30 mM, Co(NO₃)₂•6H₂O, Aldrich) and tetrabutyl ammonium chloride (1 mM, TBAC, surfactant, Aldrich), all dissolved in methanol (Aldrich). The atomic ratio of Pt to Co in the precursor solution was 1:2. Electrospinning was applied with a solution feed rate of 0.15 ml h⁻¹ and with +9 kV applied to the needle vs. a collecting substrate positioned 9 cm away. As-spun nanowires were annealed up to 500 °C in air for 90 hours to completely get rid of the PVP polymer (Figure S4). They were then reduced in H₂ at 250 °C for 5 hours to

transform into metal. The PtCo₂ nanotubes were then immersed in 1 M HNO₃ at 80 °C for 5 hours to dissolve and dealloy some Co from the surface.

Characterization. The morphologies and compositions of the catalysts were characterized by a field-emission scanning electron microscope (FESEM, Zeiss-Leo DSM982) operating at a voltage of 10 kV and by a scanning transmission electron microscope (FE(S)TEMFEI Tecnai F20) equipped with a Gatan high-angle annular dark field detector (HAADF) at an accelerating voltage of 200 kV. X-ray diffraction work was performed on a Philips X'Pert High Resolution Materials Research Diffractometer using Cu K α radiation ($\lambda=1.54$ Å). Thermogravimetric analysis was conducted on a TGA Q500 (TA Instruments), with temperature increased up to 650 °C at a rate of 10 °C min⁻¹ under sequential flows of ultra-dry high purity N₂, air and H₂.

Electrochemical measurements. Acid-leached PtCo hollow nanowires mixed with Vulcan carbon black (2 mg) were ultrasonically dispersed in a solution containing ultrapure water (1.2 mL, Milli-Q[®] system, Millipore, MA USA), 2-propanol (0.3 mL, HPLC grade, Sigma-Aldrich, USA) and Nafion[®] solution (10 μ L, 5.37%, Sigma-Aldrich, USA). Then a drop of the well-dispersed catalyst (10 μ L) was placed onto a polished glassy carbon (GC) disk electrode and dried in a gently flowing nitrogen environment for 1 h. Pt mass loading was 13.33 μ g_{Pt} cm⁻². 0.1 M HClO₄ was used as the electrolyte, diluted from 70% concentrated HClO₄ (GFS Chemicals, doubly distilled) with ultrapure water (Millipore MilliQ system). Rotating disk electrode (RDE) measurements were conducted in a 3-electrode electrochemical cell setup. Cyclic voltammograms (CVs) were measured at a scan rate of 20 mV s⁻¹ in N₂-saturated 0.1 M HClO₄. Electrochemical surface area was determined from the hydrogen adsorption area subtracted by the double layer in the CV curve, with the use of 210 μ C cm⁻² as the adsorption charge of a hydrogen monolayer. Oxygen reduction activities were measured at a rotation speed of 1600 rpm in O₂-saturated 0.1 M HClO₄ at a scan rate of 5 mV s⁻¹, all at room temperature. Durability performance was tested by potential cycling on the RDE from 0.6 to 1 V at 50 mV s⁻¹ for 10000 cycles. All the potentials in this paper are given relative to the RHE.

Conclusions

In summary, long PtCo hollow nanowires were obtained by electrospinning, annealing and acid leaching, resulting in the thinnest wall thicknesses of only 2~4 nm to our best knowledge. The temperature of reduction is found to be important to keep the hollow structure. These dealloyed hollow ultrathin nanowires showed far superior durability in terms of both resistance to surface area loss and, more importantly, activity loss when compared with commercial Pt nanoparticle catalysts.

Acknowledgements

The authors gratefully acknowledged discussions with Dr. Zhiqiang Yu, Dr. Vic Liu and James Mitchell. The experimental support from Chris Pratt and Thomas C. Jackson is appreciated. Yan Huang also thanks General Motors for financial assistance.

Notes and references

^a Materials Science Program, University of Rochester, Rochester, NY 14627, USA. E-mail address: materialsyhuang@gmail.com.

^b Electrochemical Energy Research Laboratory, GM Global R&D, Honeoye Falls, NY 14472, USA.

† Current address: Fuel Cell Institute, MOE Key Laboratory of Power & Machinery Engineering, Shanghai Jiao Tong University, Shanghai 200240, China.

Electronic Supplementary Information (ESI) available: SEM images obtained in each experimental step, size change with the time of dealloying, and TGA result. See DOI: 10.1039/b000000x/

- H. A. Gasteiger, S. S. Kocha, B. Sompalli and F. T. Wagner, *Appl. Catal. B: Environmental*, 2005, **56**, 9.
- F. Maroun, F. Ozanam, O. M. Magnussen and R. J. Behm, *Science*, 2001, **293**, 1811.
- B. C. Steele and A. Heinzel, *Nature*, 2001, **414**, 345.
- H. A. Gasteiger and N. M. Marković, *Science*, 2009, **324**, 48.
- V. R. Stamenković, B. Fowler, B. S. Mun, G. Wang, P. N. Ross, C. A. Lucas and N. M. Marović, *Science*, 2007, **315**, 493.
- E. Yeager, *Electrochim. Acta*, 1984, **29**, 1527.
- N. M. Marković, T. J. Schmidt, V. Stamenković and P. N. Ross, *Fuel Cells*, 2001, **1**, 105.
- N. M. Marković and P. N. Ross, *Surf. Sci. Rep.*, 2002, **45**, 117.
- A. Damjanovic and V. Brusic, *Electrochim. Acta*, 1967, **12**, 615.
- E. Antolini, J. R. C. Salgado and E. R. Gonnzalez, *J. Power Sources*, 2006, **160**, 957.
- S. Zhang, X. Z. Yuan, J. N. C. Hin, H. Wang, K. A. Friedrich and M. Schultz, *J. Power Sources*, 2009, **194**, 588.
- V. Rosca, M. Duca, M. T. de Groot and M. T. M. Koper, *Chem. Rev.*, 2009, **109**, 2209.
- H. Tanaka, M. Taniguchi, M. Uenishi, N. Kajita, I. Tan, Y. Nishihata, J. Mizuki, K. Narita, M. Kimura and K. Kaneko, *Angew. Chem. Int. Ed.*, 2006, **45**, 6144.
- J. B. Wu, A. Gross and H. Yang, *Nano Lett.*, 2011, **11**, 798.
- K. Jayasayee, V. Dam, T. Verhoeven, S. Celebi and F. A. Bruijn, *J. Phys. Chem. C*, 2009, **113**, 20371.
- B. Lim, M. Jiang, P. H. C. Camargo, E. C. Cho, J. Tao, X. Lu, Y. Zhu and Y. Xia, *Science*, 2009, **324**, 1302.
- S. Alayoglu, A. U. Nilekar, M. Mavrikakis and B. Elchhorn, *Nat. Mater.*, 2008, **7**, 333.
- F. Tao, M. E. Grass, Y. Zhang, D. R. Butcher, J. R. Renzas, Z. Liu, J. Y. Chung, B. S. Mun, M. Salmeron and G. A. Somorjai, *Science*, 2008, **322**, 932.
- V. R. Stamenkovic, T. J. Schmidt, P. N. Ross and N. M. Markovic, *J. Phys. Chem. B*, 2002, **106**, 11970.
- V. R. Stamenkovic, B. S. Mun, K. J. Mayrhofer, P. N. Ross and N. M. Markovic, *J. Am. Chem. Soc.*, 2006, **128**, 8813.
- M. Oezaslan, F. Hasché, P. Strasser, *J. Electrochem. Soc.*, 2012, **159**, B444.
- Y. Shao-Horn, W. C. Sheng, S. Chen, P. J. Ferreira, E. F. Holby and D. Morgan, *Top. Catal.*, 2007, **46**, 285.
- M. K. Debe, *Nature*, 2012, **486**, 43.
- P. J. Ferreira, G. J. Lao, Y. Shao-Horn, D. Morgan, R. Makharia, S. Kocha and H. A. Gasteiger, *J. Electrochem. Soc.*, 2005, **152**,

- A2256.
- 25 C. E. Carlton, S. Chen, P. J. Ferreira, L. F. Allard and Y. Shao-Horn, *J. Phys. Chem. Lett.*, 2012, **3**, 161.
- 26 Y. Yu, H. L. Xin, R. Hovden, D. Wang, E. D. Rus, J. A. Mundy, D. A. Muller and H. D. Abruna, *Nano Lett.*, 2012, **12**, 4417.
- 27 S. Chen, H. A. Gasteiger, K. Hayakawa, T. Tada and Y. Shao-Horn, *J. Electrochem. Soc.*, 2010, **157**, A82.
- 28 J. Zhang, *Front. Energy*, 2011, **5**, 137.
- 29 A. Bonakdarpour, K. Stevens, G. D. Vernstrom, R. Atanasoski, A. K. Schomeckel, M. K Debe and J. R. Dahn, *Electrochim. Acta*, 2007, **53**, 688.
- 30 M. K. Debe, A. Schmoeckel, S. Hendricks, G. Vernstrom, G. Haugen and R. Atanasoski, *ECS Trans.*, 2006, **1**, 51.
- 31 Z. W. Chen, M. Waje, W. Z. Li and Y. S. Yan, *Angew. Chem. Int. Edit.*, 2007, **46**, 4060.
- 32 J. Shui, C. Chen and J. C. M. Li, *Adv. Funt. Mater.*, 2011, **21**, 3357.
- 33 L. F. Liu and E. Pippel, *Angew. Chem. Int. Ed.*, 2011, **50**, 2729.
- 34 H. Zhou, W. P. Zhou, R. R. Adzic and S. S. Wong, *J. Phys. Chem. C*, 2009, **113**, 5460.
- 35 T. H. Yeh, C. W. Liu, H. S. Chen and K. W. Wang, *Electrochem. Commun.*, 2013, **31**, 125.
- 36 B. Y. Xia, H. B. Wu, Y. Yan, X. W. Lou and X. Wang, *J. Am. Chem. Soc.*, 2013, **135**, 9480.
- 37 C. Koenigsmann, A. C. Santulli, K. Gong, M. B. Vukmirovic, W. Zhou, E. Sutter, S. S. Wong and R. R. Adzic, *J. Am. Chem. Soc.*, 2011, **133**, 9783.
- 38 L. Liu, E. Pippel, R. Scholz and U. Gosele, *Nano Lett.*, 2009, **9**, 4352.
- 39 S. W. Chou, J. J. Shyue, C. H. Chien, C. C. Chen, Y. Y. Chen, P. T. Chou, *Chem. Mater.*, 2012, **24**, 2527.
- 40 H. Liao and Y. Hou, *Chem. Mater.*, 2013, **25**, 457.
- 41 S. M. Alia, K. Jensen, C. Contreras, F. Garzon, B. Pivovar and Y. Yan, *ACS Catal.*, 2013, **3**, 358.
- 42 H. Zhu, S. Zhang, S. Guo, D. Su and S. Sun, *J. Am. Chem. Soc.*, 2013, **135**, 7130.
- 43 S. Sun, G. Zhang, D. Geng, Y. Chen, M. N. Banis, R. Li, M. Cai and X. Sun, *Chem. Eur. J.*, 2010, **16**, 829.
- 44 B. Luo, X. Yan, J. Chen, S. Xu and Q. Xue, *Int. J. Hydrogen Energy*, 2013, **38**, 13011.
- 45 H. H. Li, C. H. Cui, S. Zhao, H. B. Yao, M. R. Gao, F. J. Fan and S. H. Yu, *Adv. Energy Mater.*, 2012, **2**, 1182.
- 46 J. Kim, S. W. Lee, C. Carlton and Y. Shao-Horn, *J. Phys. Chem. Lett.*, 2011, **2**, 1332.
- 47 W. Zhang, A. I. Minett, M. Gao, J. Zhao, J. M. Razal, G. G. Wallace, T. Romeo and J. Chen, *Adv. Energy Mater.*, 2011, **1**, 671.
- 48 M. B. Ishaq and F. Patolsky, *J. Am. Chem. Soc.*, 2011, **133**, 1545.
- 49 T. Li, S. Yang, L. Huang, B. Gu and Y. Du, *Nanotechnology*, 2004, **15**, 1479.
- 50 J. L. Shui, J. W. Zhang and J. C. M. Li, *J. Mater. Chem.*, 2011, **21**, 6225.
- 51 J. L. Shui and J. C. M. Li, *Nano Lett.*, 2009, **9**, 1307.
- 52 M. Bognitzki, M. Becker, M. Graeser, W. Massa, J. H. Wendorff, A. Schaper, D. Weber, A. Beyer, A. Golzhauer and A. Greiner, *Adv. Mater.*, 2006, **18**, 2384.
- 53 H. Wu, R. Zhang, X. X. Liu, D. D. Lin and W. Pan, *Chem. Mater.*, 2007, **19**, 3506.
- 54 V. G. Pol, E. Koren and A. Zaban, *Chem. Mater.*, 2008, **20**, 3055.
- 55 J. M. Kim, H. I. Joh, S. M. Jo, D. J. Ahn, H. Y. Ha, S. A. Hong and S. K. Kim, *Electrochim. Acta*, 2010, **55**, 4827.
- 56 H. J. Kim, Y. S. Kim, M. H. Seo, S. M. Choi and W. B. Kim, *Electrochem. Commun.*, 2009, **11**, 446.
- 57 X. Chen, K. M. Unruh, C. Ni, B. Ali, Z. Sun, Q. Lu, J. Deitzel and J. Q. Xiao, *J. Phys. Chem. C*, 2011, **115**, 373.
- 58 D. J. Guo and S. K. Cui, *J. Colloid Interface Sci.*, 2009, **340**, 53.
- 59 J. W. Hong, S. W. Kang, B. S. Choi, D. Kim, S. B. Lee and S. W. Han, *ACS Nano*, 2012, **6**, 2410.
- 60 H. Xiang, Y. Long, X. Yu, X. Zhang, N. Zhao and J. Xu, *CrystEngComm*, 2011, **13**, 4856.
- 61 Z. Shen, Y. Wang, W. Chen, L. Fei, K. Li, H. Lai, W. Chan and L. Bing, *J. Mater. Sci.*, 2013, **48**, 3985.
- 62 Y. Ding, C. Hou, B. Li and Y. Lei, *Electroanalysis*, 2011, **23**, 1245.
- 63 J. Liu, K. Song, P. A. van Aken, J. Maier and Y. Yu, *Nano Lett.*, 2014, **14**, 2597.
- 64 V. R. Stamenkovic, B. S. Mun, M. Arenz, K. J. J. Mayrhofer, C. A. Lucas, G. Wang, P. N. Ross and N. M. Markovic, *Nat. Mater.*, 2007, **6**, 241.
- 65 Y. Huang, J. Zhang, A. Kongkanand, F. T. Wagner, J. C. M. Li and J. Jorné, *J. Electrochem. Soc.*, 2014, **161**, F10.
- 66 S. Sun, G. Zhang, D. Geng, Y. Chen, R. Li, M. Cai, and X. Sun, *Angew. Chem. Int. Ed.* 2011, **50**, 422-426.
- 67 Z. Chen, M. Waje, W. Li, and Y. Yan, *Angew. Chem. Int. Ed.* 2007, **46**, 4060-4063.
- 68 M. K. Debe, S. M. Hendricks, G. D. Vernstrom, M. Meyers, M. Brostrom, M. Stephens, Q. Chan, J. Willey, M. Hamden, C. K. Mittelsteadt, C. B. Capuano, K. E. Ayers, and E. B. Anderson, *J. Electrochem. Soc.* 2012, **159**, K165-K176.
- 69 H. W. Liang, X. Cao, F. Zhou, C. H. Cui, W. J. Zhang, and S. H. Yu, *Adv. Mater.* 2011, **23**, 1467-1471.
- 70 L. Ruan, E. Zhu, Y. Chen, Z. Lin, X. Huang, X. Duan, and Y. Huang, *Angew. Chem. Int. Ed.* 2013, **52**, 12577-12581.
- 71 L. Liu, E. Pippel, R. Scholz, and U. Gösele, *Nano Lett.* 2009, **9**, 4352-4358.
- 72 L. Liu, R. Scholz, E. Pippel, and U. Gösele, *J. Mater. Chem.* 2010, **20**, 5621-5627.
- 73 S. M. Alia, B. A. Larsen, S. Pylypenko, D. A. Cullen, D. R. Diercks, K. C. Neyerlin, S. S. Kocha, and B. S. Pivovar, *ACS Catal.* 2014, **4**, 1114-1119.
- 74 S. Guo, S. Zhang, D. Su, and S. Sun, *J. Am. Chem. Soc.* 2013, **135**, 13879-13884.
- 75 K. Sasaki, H. Naohara, Y. Cai, Y. M. Choi, P. Liu, M. B. Vukmirovic, J. X. Wang and R. R. Adzic, *Angew. Chem. Int. Ed.*, 2010, **49**, 8602.
- 76 Y. Shao, G. Yin and Y. Gao, *J. Power Sources*, 2007, **171**, 558.
- 77 E. Antolini, J. R.C. Salgado, and E. R. Gonzalez, *Journal of Power Sources* 2006, **160**, 957-968.
- 78 H. R. Colon-Mercado, and B. N. Popov, *Journal of Power Sources* 2006, **155**, 253-263.
- 79 P. Yu, M. Pemberton, and P. Plasse, *Journal of Power Sources* 2005, **144**, 11-20.
- 80 S. C. Zignani, E. Antolini, and E. R. Gonzalez, *Journal of Power Sources* 2008, **182**, 83-90.
- 81 K. W. Nam, J. Song, K. H. Oh, M. J. Choo, H. Park, J. K. Park, and

- J. W. Choi, *Carobn* 2012, **50**, 3739-3747.
- 82 Q. Xu, E. Kreidler, T. He, *Electrochimica Acta* 2010, **55**, 7551-7557.
- 83 S. M. Alia, G. Zhang, D. Kisailus, D. S. Li, S. Gu, K. Jensen and Y. S. Yan, *Adv. Funct. Mater.*, 2010, **20**, 3742.
- 84 S. H. Sun, G. X. Zhang, D. S. Geng, Y. G. Chen, R. Y. Li, M. Cai and X. L. Sun, *Angew. Chem. Int. Ed.*, 2011, **50**, 422.

